https://doi.org/10.15415/jnp.2018.52023

Distinguishing Features of Radioactive Compound Nucleus Decays within the Dynamical Cluster-decay Model

HEMDEEP[1,*], SAHILA CHOPRA, POOJA KAUSHAL AND RAJ K. GUPTA

Department of Physics, Panjab University, Chandigarh, India-160014

[1,*]**Email: hemdeep08@gmail.com**

Received: December 18, 2017| Revised: January 09, 2018| Accepted: January 20, 2018

Published online: February 5, 2018

Abstract In this paper, we are interested to study the distinguishing features of the decaying radioactive compound nuclei $^{246}Bk^*$ and $^{220}Th^*$, using the Dynamical Cluster-decay Model (DCM) with deformation β and non-coplanar degree-of-freedom Φ. $^{246}Bk^*$ and $^{220}Th^*$ have so-far been studied within the DCM, using quadrupole deformations (β_{2i}), “optimum” orientations (θ^{opt}) of the two nuclei lying in the same plane ($\Phi=0^o$), which shows that there is a non-compound nucleus (nCN) content in the observed data. The first turning point R_a (equivalently, the neck-length ΔR in $R_a=R_1+R_2+\Delta R$), which fixes both the preformation and penetration paths, is used to best fit the measured evaporation residue (ER) and fusion-fission (ff) cross sections, σ_{ER}, σ_{ff}, respectively, in $^{220}Th^*$ and $^{246}Bk^*$, formed via different entrance channels. In this work, we subsequently add higher multipole deformations, the octupole and hexadecupole (β_{3i}, β_{4i}), `compact’ orientations θ_{ci} and $\Phi\neq0^0$, and look for their effects on the nCN contribution predicted by the DCM calculations referenced above.

Keywords: Dynamical cluster-decay model; deformed non-coplanar fragments; non-compound nucleus effects; radioactive nuclei.

1. INTRODUCTION

Heavy-ion reactions present themselves as the best tools to study the nuclear reaction-mechanism and structure of nuclei. Our present study comprises the radioactive $^{220}Th^*$ and $^{246}Bk^*$ compound nuclei (CN) formed through different entrance channels, worked out within the Dynamical Cluster-decay Model (DCM). Gupta and collaborators [1-3] studied the case of CN $^{246}Bk^*$ formed

Journal of Nuclear Physics, Material Sciences, Radiation and Applications
Vol-5, No-2, February 2018
pp. 255–263

through $^{11}B+^{235}U$ and $^{14}N+^{232}Th$ channels, where the DCM calculations with quadrupole deformations (β_{2i}) and "optimum" orientations (θ^{opt}) of the two nuclei lying in the same plane (co-planar nuclei, azimuthal angle $\Phi=0^o$), showed that for $^{11}B+^{235}U$ channel an amount of non-compound nucleus (nCN) contribution is required but for $^{14}N+^{232}Th$ channel it is a pure CN decays. More recently, the same DCM calculations for $^{220}Th^*$ [4] formed via entrance channels $^{16}O+^{204}Pb$, $^{40}Ar+^{180}Hf$, $^{48}Ca+^{172}Yb$ and $^{82}Se+^{138}Ba$, using β_{2i} alone with θ^{opt} and $\Phi=0^o$, show that the 3n and 5n decay channels are pure CN decay, but the 4n channel required an amount of nCN content treated as a quasi-fission (qf) process. In the present work, we subsequently add the higher multipole deformations, i.e., octupole and hexadecupole (β_{3i}, β_{4i}) deformations with corresponding "compact" orientations θ_{ci} and non-coplanarity degrees-of-freedom ($\Phi \neq 0^o$). With inclusion of $\beta_{2i}-\beta_{4i}$, we notice that the "compact" orientation angles θ_{ci}, calculated as per prescription [5], change by as much as 36^o and the "compact" Φ_c by as much as 34^o for light-particles decays of $^{220}Th^*$ CN. The interesting point now is to see the effect of such large changes in θ_{ci} on potential energy surfaces, etc., for the reactions $^{48}Ca+^{172}Yb$ [6] and $^{40}Ar+^{180}Hf$ [7] studied for $^{220}Th^*$. Note that here, the targets ^{172}Yb and ^{180}Hf belong to strongly deformed rare-earth region which are expected [8] to contain the nCN decay effects, also studied recently in $^{48}Ca+^{154}Gd\rightarrow^{202}Po^*$ reaction both experimentally [9] and theoretically [10]. On the other hand, for $^{246}Bk^*$, both the CN and target nuclei in channels $^{11}B+^{235}U$ and $^{14}N+^{232}Th$ are from strongly deformed radioactive actinide region.

A brief description of the Quantum Mechanical Fragmentation Theory (QMFT)-based Dynamical Cluster-decay Model (DCM) is presented in Section 2, and our calculations and results discussed in Section 3, followed by a Summary in Section 4.

2. METHODOLOGY

The DCM [11,12] for the decay of hot and rotating CN is worked out in terms of relative separation coordinate R, mass (and charge) asymmetries $\eta=(A_1-A_2)/(A_1+A_2)$ [and $\eta_Z = (Z_1-Z_2)/(Z_1+Z_2)$], multipole deformations $\beta_{\lambda i}$ (λ=2,3,4; i=1,2), orientations θ_i and the azimuthal angle Φ between the principal planes of two nuclei, shown in Fig. 1 for the co-planar $\Phi=0^o$ case. In terms of these coordinates, for ℓ partial waves, we define the CN decay/ production cross section for each fragment as

$$\sigma_{(A_1,A_2)} = \sum_{\ell=0}^{\ell_{max}} \sigma_\ell = \frac{\pi}{k^2}\sum_{\ell=0}^{\ell_{max}}(2\ell+1)P_0P; \quad k=\sqrt{\frac{2\mu E_{c.m.}}{\hbar^2}} \tag{1}$$

where, P_0, the pre-formation probability, refers to η-motion and P, the penetrability, to R-motion, both depending on ℓ, T, $\beta_{\lambda i}$, θ_i and Φ.

The P_0 is the solution of stationary Schrödinger equation in η, at a fixed $R=R_a$, the first turning point(s) of the penetration path(s) for different ℓ-values,

$$\left\{-\frac{\hbar^2}{2\sqrt{B_{\eta\eta}}}\frac{\partial}{\partial\eta}\frac{1}{\sqrt{B_{\eta\eta}}}\frac{\partial}{\partial\eta}+V_R(\eta)\right\}\Psi_R^{(\nu)}(\eta)=E_R^{(\nu)}\Psi_R^{(\nu)}(\eta) \quad (2)$$

with $\nu = 0,1,2,3....$, referring to ground-state ($\nu = 0$) and excited-state solutions. Then, preformation

$$P_0(A_i)=|\psi_R(\eta(A_i))|^2\sqrt{B_{\eta\eta}}\frac{2}{A} \quad (3)$$

Here, $B_{\eta\eta}$, the mass parameters, are the smooth classical hydrodynamical masses [14], used for simplicity. In principle, one should use the cranking masses, based on the underlying shell model prescription.

For the first turning point R_a, in the case of the decay of a hot CN, we use the postulate [13]

$$R_a = R_1(\alpha_1,T)+R_2(\alpha_2,T)+\Delta R(\eta,T) \quad = R_t(\alpha,\eta,T)+\Delta R(\eta,T) \quad (4)$$

with radius vectors $R_i(\alpha_i,T)=R_{0i}(T)\left[1+\sum_\lambda \beta_{\lambda i}Y_\lambda^{(0)}(\alpha_i)\right]$ and the temperature dependent nuclear radii $R_{0i}(T)$, for the equivalent spherical nucleus (see Fig. 1, for the definition of angles α's, etc.),

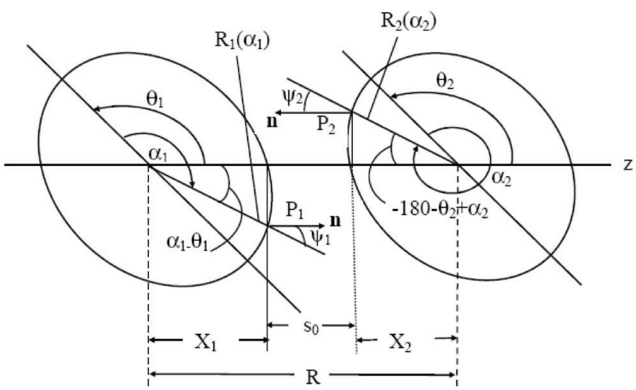

Figure 1: Schematic configuration of any two axially symmetric, deformed, oriented nuclei, lying in the same plane ($\Phi=0^0$), based on Fig. 1 in [13].

$$R_{0i} = [1.28A_i^{1/3} - 0.76 + 0.8A_i^{-1/3}](1 + 0.0007T^2) \tag{5}$$

The penetrability P in Eq. (1) is the WKB integral,

$$P = \exp\left[-\frac{2}{\hbar} \int_{R_a}^{R_b} \left\{ 2\mu \left[V(R,T) - Q_{eff} \right] \right\}^{1/2} dR \right] \tag{6}$$

solved analytically [15] with the second turning point R_b satisfying $V(R_a)=V(R_b)=Q_{eff}=TKE(T)$ (see, Fig. 2 in Ref. [4]). This means that $V(R_a,\ell)$ acts like an effective Q-value, $Q_{eff}(T,\ell)$, given by the total kinetic energy TKE(T).

The collective fragmentation potential $V_R(\eta, T)$ in Eq. (2), that brings in the structure effects of the CN in to the formalism, is calculated according to the Strutinsky renormalization ($B = V_{LDM} + \delta U$; B is binding energy) procedure as,

$$V_R(\eta, T) = \sum_{i=1}^{2}[V_{LDM}(A_i, Z_i, T)] + \sum_{i=1}^{2}[\delta U_i]\exp\left(-\frac{T^2}{T_0^2}\right) + V_P(R, A_i, \beta_{\lambda i}, \theta_i, T) + V_C(R, Z_i, \beta_{\lambda i}, \theta_i, T) + V_\ell(R, A_i, \beta_{\lambda i}, \theta_i, T) \tag{7}$$

Here, the macroscopic part V_{LDM} of binding energy $B(A_i,Z_i,T)$ is temperature (T) dependent liquid drop energy of Davidson *et al.* [16] with its constants

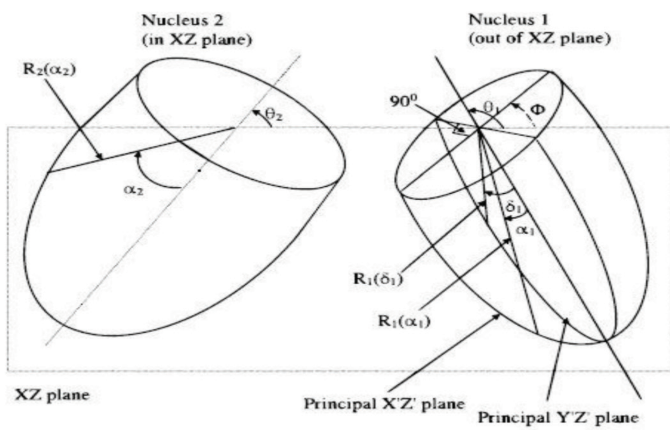

Figure 2: The same as for Fig. 1, but for non-coplanar nuclei ($\Phi\neq0^0$), based on Fig. 1 in [24].

at T=0 refitted by some of us [1, 12, 17] to give the experimental binding energies B, done more recently [1] for the 2003 Tables of Audi *et al.* [18], used here. Whenever the experimental B were not available, the theoretical estimates of Möller *et al.* [19] are used. The microscopic shell corrections part δU are the "empirical" estimates of Myers and Swiatecki [20] for spherical nuclei, also taken T-dependent, i.e., $\delta U(T) = \delta U \exp(-T^2/T_0^2)$ with $T_0=1.5$ MeV [21]. This means that the shell correction term $\delta U(T)$ becomes nearly zero for T>4 MeV. The shell effects are also known to depend strongly on the deformation of a nucleus but a similar prescription for deformed nuclei is not available. However, here these effects are included to some extent in V_{LDM}, since we essentially use the experimental binding energies [18] split into two contributions, V_{LDM} and δU, with constants of V_{LDM} at T=0 fitted to experimental binding energies. The T-dependence is also included in nuclear proximity potential V_P (Blocki *et al.* pocket formula), Coulomb V_C and ℓ-dependent potential V_ℓ, for deformed, oriented nuclei [22, 23].

The same formalism as above is used for non-coplanar nuclei ($\Phi \neq 0^o$, see Fig. 2), but by replacing for the out-of-plane nucleus (i = 1 or 2), the corresponding radius parameter $R_i(\alpha_i)$ with its projected radius parameter $R_i^P(\alpha_i)$ in both the Coulomb and proximity potentials in Eq. (2). For the proximity potential, it enters via the definitions of both the mean curvature radius $\bar{R}$ and the shortest distance s_0 (see Ref. [24]). The $R_i^P(\alpha_i)$ is determined by defining, for the out-of-plane nucleus, two principal planes *X'Z'* and *Y'Z'*, respectively, with radius parameters $R_i(\alpha_i)$ and $R_j(\delta_j)$, such that their projections into the plane *XZ* of the other nucleus are

$$R_i^P(\alpha_i) = R_i(\alpha_i)\cos\Phi \qquad (i = 1 \text{ or } 2) \tag{8}$$

and

$$R_j^P(\delta_j) = R_j(\delta_j)\cos(\Phi - \delta_j) \qquad (j = i = 1 \text{ or } 2) \tag{9}$$

Then, maximizing $R_j(\delta_j)$ in angle δ_j, we get

$$\begin{aligned} R_i^P(\alpha_i) &= R_i^P(\alpha_i = 0) + R_i^P(\alpha_i \neq 0) \\ &= R_j^P(\delta_j^{\max}) + R_i(\alpha_i \neq 0)\cos\Phi \end{aligned} \tag{10}$$

with $\delta_j^{\max}$ given by the condition (for fixed Φ),

$$\tan(\Phi - \delta_j) = -\frac{R_1^{'}(\delta_j)}{R_1(\delta_j)} \qquad (11)$$

Apparently, the Φ-dependence of the projected radius vector $R_j^P(\alpha_i)$ is also contained in maximized $R_j^P(\delta_j^{max})$. For further details, see Ref. [24]. Then, denoting by V_P^{12} the nuclear proximity potential for the nucleus 1 to be out-of-plane, and by V_P^{21} for the nucleus 2 to be out-of-plane, the effective nuclear proximity potential can be approximated by $V_P=1/2[V_P^{12}+V_P^{21}]$. Note, for co-planar and identical (both nuclei same) non-coplanar nuclei $V_P^{12}=V_P^{21}$.

3. CALCULATIONS AND RESULTS

For making a comparative study of the decaying $^{246}Bk^*$ and $^{220}Th^*$ radioactive CN and their distinguishing features, Fig. 3 shows our DCM calculated decay-channel cross sections for (a) $^{246}Bk^*$ and (b) $^{220}Th^*$, each for two different entrance channels at a fixed CN excitation energy E_{CN}^* for the three cases of β_{2i}-alone with θ^{opt} and co-planar nuclei $\Phi=0^o$, the β_{2i}-β_{4i}, θ_{ci}, $\Phi=0^o$ and $\Phi\neq0^o$ cases, together with the available experimental data. Here, the scattering potential V(R) and fragmentation potential V(η), like the ones in Figs. (2) and (8) of Ref. [4], are calculated for fixed R_a (equivalently, fixed neck-length ΔR in $R_a=R_1+R_2+\Delta R$), which fixes both the penetration and preformation paths, for a best fit of the observed decay-channel cross sections (σ_{ff} for $^{246}Bk^*$ and σ_{xn}, x=3-5 for $^{220}Th^*$), keeping the root-mean square (r.m.s) deviation between the calculated and experimental decay-channel cross section, at each E_{CN}^*, to a minimum value. Such calculations for the radioactive CN $^{246}Bk^*$ formed through $^{11}B+^{235}U$ and $^{14}N+^{232}Th$ entrance channels by Gupta and collaborators [1-3], using quadrupole deformations β_{2i}-alone, θ^{opt} and $\Phi=0^o$, show the presence of quasi-fission (qf)-like nCN component in fission cross section of $^{11}B+^{235}U$ channel, but not in $^{14}N+^{232}Th$ channel (see, Fig. 3(a)). Here, the (qf-like) nCN component is defined as the measure of disagreement between the calculated and measured fission cross section, taken as a measure of fusion cross section σ_{fus}. Interestingly, however, with higher-multipole deformations β_{2i}- β_{4i}, "compact" orientations θ_{ci}, and Φ not-included ($\Phi=0^0$) or included ($\Phi\neq0^o$), the nCN contribution in $^{14}N+^{232}Th$ channel remains the same, i.e., zero nCN, but for $^{11}B+^{235}U\rightarrow^{246}Bk^*$ reaction also, the nCN content get reduced to zero successively, at all E_{CN}^*. Thus, the predicted nCN in $^{246}Bk^*$ for entrance channel $^{11}B+^{235}U$ is simply an artefact of our calculations of including/ or not-including β_{2i}-β_{4i} with θ_{ci} and non-coplanarity Φ.

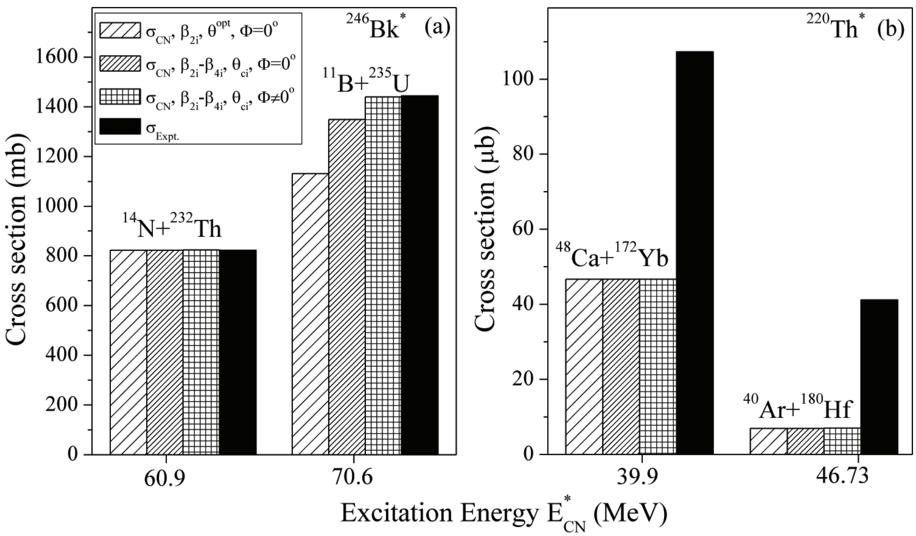

Figure 3: DCM calculated CN cross sections for (a) ^{246}Bk* (b) ^{220}Th*, for different entrance channels, compared with experimental data. These calculations are for the three cases of (i) β_{2i}-alone with θ^{opt} and co-planar nuclei $\Phi=0^o$, (ii) β_{2i}-β_{4i}, θ_{ci}, $\Phi=0^o$ and (iii) β_{2i}-β_{4i}, θ_{ci}, $\Phi\neq0^o$.

Recently, the DCM calculations for ^{220}Th* [4], formed through the entrance channels ^{40}Ar+^{180}Hf and ^{48}Ca+ ^{172}Yb, using β_{2i} alone, "optimum" orientation θ^{opt} and co-planar nuclei $\Phi=0^o$ show that there is an nCN contribution in the observed 4n decay channel, but the 3n and 5n decay channels fit the data as pure CN decays. Note that, in these reactions, the targets ^{172}Yb and ^{180}Hf belong to lanthanide region of strongly deformed rare-earth nuclei, which are expected to contain the nCN decay effects. Figure 3(b) shows the interesting result in case of CN ^{220}Th*, relative to the ones above for ^{246}Bk*, both being radioactive nuclei, that with the inclusion of β_{2i}-β_{4i}, θ_{ci}, $\Phi=0^o$ or $\Phi\neq0^o$, there is still the same amount of nCN contribution present in 4n decay channel which could not be reduced/ or removed. In other words, it seems that the nCN contribution in ^{220}Th* is real, and, unlike ^{246}Bk*, not an artefact of our calculations.

Thus, the above result seems to suggest either the significance of $\beta_{\lambda i}$ (λ=2-4) and Φ degrees-of-freedom in oriented heavy ion reactions, or that it is the characteristic, distinguishing features of the chosen entrance channels or of the decaying compound nucleus. Note that the entrance channels for ^{246}Bk* refer to very asymmetric target-projectile combinations with targets from strongly deformed actinide region, and that the ones for ^{220}Th* refer to targets from deformed rare-earth region.

Hemdeep,
Chopra, S
Kaushal, P
Gupta, RK

4. SUMMARY AND CONCLUSIONS

In this paper, we have made a comparative study of two decaying radioactive compound nuclei $^{220}Th^*$ and $^{246}Bk^*$ from the point of view of including/ or not-including the higher multi-pole deformations (β_{3i}, β_{4i}), "compact" orientations (θ_{ci}) of two nuclei with non-coplanarity **(Φ)** also as the degree-of-freedom, and looked for their effects on the nCN cross section. In the case of $^{246}Bk^*$, the $\beta_{\lambda i}$ (λ=2-4) or non-coplanarity degree-of-freedom Φ nullifies the nCN contribution observed in the β_{2i}-alone with $\Phi=\mathbf{0}^o$ case, showing both the reaction channels as pure CN decays. On the other hand, for the case of $^{220}Th^*$ there is no change in the nCN contribution and thus manifests the presence of nCN content in CN formed through deformed rare-earth targets. Experimental verification is called for.

Concluding, deformations of nuclei, including higher multi-poles, i.e., $\beta_{\lambda i}$ (λ=2-4), their compact orientations and non-coplanarity Φ show their importance in heavy-ion reactions via the nCN content in pure CN decays.

ACKNOWLEDGEMENTS

Work supported in parts by the University Grants Commission (UGC), New Delhi, in terms of a Senior Research Fellowship for one of us (Hemdeep), and by the Science and Engineering Research Board (SERB) of Department of Science and Technology (DST), Govt. of India, New Delhi, in terms of the Research Project No. EMR/2016/001131 to RKG.

REFERENCES

[1] B. B. Singh, M. K. Sharma, and R. K. Gupta, Phys. Rev. C **77,** 054613 (2008). https://doi.org/10.1103/PhysRevC.77.054613

[2] R. K. Gupta and M. Bansal, Int. Rev. of Phys. (I.RE.PHY) **5,** 74 (2011).

[3] M. Bansal, Ph.D. Thesis, Panjab University, Chandigarh, (2012).

[4] Hemdeep, S. Chopra, A. Kaur, and R. K. Gupta, Phys. Rev. C **95,** 014609 (2017). https://doi.org/10.1103/PhysRevC.95.014609

[5] R. K. Gupta, M. Manhas and W. Greiner, Phys. Rev. C **73,** 054307 (2006). https://doi.org/10.1103/PhysRevC.73.054307

[6] C. C. Sahm, et al., Nucl. Phys. A **441,** 316 (1985). https://doi.org/10.1016/0375-9474(85)90036-3

[7] D. Vermeulen, et al., Z. Phys. A **318,** 157 (1984). https://doi.org/10.1007/BF01413464

[8] G. N. Knyazheva, et al., Phys. Rev. C **75,** 064602 (2007). https://doi.org/10.1103/PhysRevC.75.064602

[9] D. A. Mayorov, et al., Phys. Rev. C **90,** 024602 (2014).
https://doi.org/10.1103/PhysRevC.90.024602

[10] P. Kaushal, S. Chopra, Hemdeep, and R. K. Gupta, Proceedings DAE-BRNS Symposium on Nucl. Phys. **62,** 480 (2017).

[11] R. K. Gupta, in Clusters in Nuclei, Lecture Notes in Physics 818, edited by C. Beck, **Vol. I**, (Springer Verlag, Berlin, 2010), pp. 223–265.

[12] R. K. Gupta, R. Kumar, N. K. Dhiman, M. Balasubramaniam, W. Scheid, and C. Beck, Phys. Rev. C **68,** 014610 (2003).
https://doi.org/10.1103/PhysRevC.68.014610

[13] R. K. Gupta, M. Balasubramaniam, R. Kumar, N. Singh, M. Manhas, and W. Greiner, J. Phys. G: Nucl. Part. Phys. **31,** 631 (2005).
https://doi.org/10.1088/0954-3899/31/7/009

[14] H. Kroeger and W. Scheid, J. Phys. G **6,** L85 (1980).
https://doi.org/10.1088/0305-4616/6/4/006

[15] S. S. Malik and R. K. Gupta, Phys. Rev. C **39,** 1992 (1989).
https://doi.org/10.1103/PhysRevC.39.1992

[16] N. J. Davidson, S. S. Hsiao, J. Markram, H. G. Miller, and Y. Tzeng, Nucl. Phys. A **570,** 61c (1994). https://doi.org/10.1016/0375-9474(94)90269-0

[17] M. Balasubramaniam, R. Kumar, R. K. Gupta, C. Beck, and W. Scheid, J. Phys. G: Nucl. Part. Phys. **29,** 2703 (2003). https://doi.org/10.1088/0954-3899/29/12/003

[18] G. Audi, A. H. Wapstra, and C. Thiboult, Nucl. Phys. A **729,** 337 (2003).
https://doi.org/10.1016/j.nuclphysa.2003.11.003

[19] P. Möller, J. R. Nix, W. D. Myers, and W. J. Swiatecki, At. Data Nucl. Data Tables **59,** 185 (1995)

[20] W. Myers and W. J. Swiatecki, Nucl. Phys. **81,** 1 (1966).
https://doi.org/10.1016/0029-5582(66)90639-0

[21] S. Jensen and J. Damgaard, Nucl. Phys. A, **203,** 578 (1973).
https://doi.org/10.1016/0375-9474(73)90365-5

[22] R. K. Gupta, N. Singh, and M. Manhas, Phys. Rev. C **70,** 034608 (2004).
https://doi.org/10.1103/PhysRevC.70.034608

[23] S. Chopra, M. Bansal, M. K. Sharma, and R. K. Gupta, Phys. Rev. C **88,** 014615 (2013). https://doi.org/10.1103/PhysRevC.88.014615

[24] M. Manhas and R. K. Gupta, Phys. Rev. C 72, 024606 (2005).
https://doi.org/10.1103/PhysRevC.72.024606